Formation and magnetic properties of $Sm_3(Fe,Ti)_{29}N_y$ compounds

Formation and magnetic properties of $Sm_3(Fe,Ti)_{29}N_y$ compounds

Yang Fuming†, B Nasunjilegal†, Wang Jianli†, Zhu Jianjun†, Qin Weidong†, N Tang†, Zhao Ruwen†, Bo-Ping Hu‡, Yi-Zhong Wang‡ and Hong-Shuo Li§

† Magnetism Laboratory, Institute of Physics, Chinese Academy of Sciences, PO Box 603, Beijing 100080, People's Republic of China
‡ San Huan Research Laboratory, Chinese Academy of Sciences, PO Box 603, Beijing 100080, People's Republic of China
§ School of Physics, University of New South Wales, Kensington 2033, Australia

Abstract. The formation and magnetic properties of a novel intermetallic $Sm_3(Fe_{0.933}Ti_{0.067})_{29}$ compound and the $Sm_3(Fe_{0.933}Ti_{0.067})_{29}N_y$ $(y = 5)$ nitride have been investigated. The x-ray diffraction patterns of the nitride and the parent compound were indexed on the basis of the $Nd_3(Fe,Ti)_{29}$-type structure with monoclinic symmetry. The parent and the nitride exhibit ferromagnetic ordering with a Curie temperature T_C of 486 K for the parent and 750 K for the nitride. Introduction of nitrogen led to an increase in saturation magnetization; M_s for the nitride is 160 A m² kg⁻¹ at 4.2 K and 140 A m² kg⁻¹ at 293 K. The nitride has a uniaxial anisotropy with an anisotropy field strength B_a for 25 T at 4.2 K and 12.8 T at 293 K. The coercivity $\mu_0 H_c = 0.83$ T at 293 K for this new nitride has been determined.

1. Introduction

The discovery of the $Nd_2Fe_{14}B$ compound [1] not only has led to the appearance of a new generation of the rare-earth permanent magnets, having outstanding permanent magnetic performances, but also has stimulated researchers to search for novel iron-rich rare-earth–transition-metal intermetallic compounds as permanent magnet materials.

In continuing research for new permanent magnetic materials, first of all the attention was focused on the investigation of the magnetic properties of the $R(Fe,T)_{12}$ compounds with $ThMn_{12}$-type (1:12) structure, where $R \equiv$ rare earth or Y, and T is a stabilizing element because the RFe_{12} phase does not exist. It was found that T could be Ti, V, Cr, Si, Mo, W, etc. Of these, $Sm(Fe,Ti)_{12}$ seemed to be the most potentially useful candidate [2]. Later it was found that the Sm_2Fe_{17} carbides [3] and nitrides [4] with Th_2Zn_{17}-type (2:17) structure, and $Nd(Fe,Ti)_{12}$ nitrides [5] show excellent intrinsic permanent magnetic properties. On the other hand, the search for a new phase and new compounds is still continuing. It has been found that the $Sm_{11}Fe_{79}Si_{10}$ nitride with $SmFe_5$ phase (1:5) exhibits excellent intrinsic permanent magnetic properties [6]. There have also been many reports on the new rare-earth–iron compounds with 1:7 phase [7–10].

Recently a new ternary phase $Nd_2(Fe,Ti)_{19}$ and a similar phase $R_2(Fe_{0.91}V_{0.09})_{19}$ ($R \equiv$ Y, Nd, Sm or Gd) were discovered by Collocott *et al* [11] and Shcherbakova *et al* [12], respectively. These workers used the superstructure of $CaCu_5$ type to index the x-ray diffraction patterns obtained in the new phase. Very recently, the new magnetic ternary rare-earth iron-rich intermetallic compound, previously reported as $Nd_2(Fe,Ti)_{19}$, has been

identified to be a $Nd_3(Fe,Ti)_{29}$-type structure. The structure consists of 15 unique transition-metal sites and two rare-earth sites, in a monoclinic cell of symmetry $P2_1/c$ [13, 14].

In order to obtain a material which can be used for permanent magnet applications, the material is required to exhibit uniaxial anisotropy and to have a saturation magnetization which is as high as possible. So we have chosen Sm for which the second Stevens coefficient α_J is positive and Ti as a stabilizing element. A new $Sm_3(Fe,Ti)_{29}$ compound with a single phase which has a nitride with outstanding intrinsic permanent magnetic properties has been obtained. In this paper we report the formation, structure and magnetic properties of a novel $Sm_3(Fe,Ti)_{29}$ compound and its nitride, and also preliminary results from a study of the hard magnetic properties associated with the novel $Sm_3(Fe,Ti)_{29}N_y$ magnet.

2. Experimental details

Ingots of $Sm_{10}Fe_{85}Ti_x$ with $x = 4.2$, 4.4, 4.6, 4.8, 5.0, 6.0 and 6.5 were prepared by argon arc melting starting elements of purity at least 99.9%. The ingots were melted in the water-cooled copper hearth and remelted at least twice to promote mixing. Subsequently, the ingots were annealed in vacuum at 1273–1473 K for 10–60 h, wrapped in molybdenum foil and sealed in quartz tubes, followed by quenching in air or in water. An excess amount of Sm was added to compensate for the loss of the Sm during the melting. In order to prepare nitrides the ingots were pulverized into fine powders with an average size of 15 μm. The gas-phase reaction between the alloys and nitrogen was studied by thermopiezoelectric analysis [15]. The nitrogenation of a large number of samples was performed by heating the fine powders in nitrogen at 1 atm at a temperature between 770 and 870 K for about 2 h. The nitrogen content was determined from the difference between the mass before and that after nitrogenation.

The nitride powders were then ball milled using metal balls of 4–10 mm diameter with a sample-to-metal-balls weight ratio of 1 to 60. The samples for the magnetic measurements were made by mixing the ball-milled nitride powder with epoxy resin, solidifying in an applied field strength of 2 T at room temperature. X-ray diffraction with Co $K\alpha$ radiation was employed to determine the phase of the alloys and the lattice parameters. X-ray diffraction patterns of the magnetically aligned powder samples obtained at room temperature were used to determine the easy magnetization direction of the nitrides and the parent compounds. The thermomagnetic analysis ($\sigma(T)$) in a low field strength of 0.04 T was performed from room temperature to about 800 K. The Curie temperature T_C was determined from σ^2–T plots by extrapolating σ^2 to zero. The magnetization curves $\sigma(B)$ were measured by means of a SQUID magnetometer and an extracting-sample magnetometer with applied field strengths of up to 7 T, or by pulsed magnetic field strengths up to 20 T at temperatures ranging from 77 K to room temperature. The high-field magnetization curves in applied field strengths up to 35 T were measured at 4.2 K in the High-Field Installation at the University of Amsterdam [16]. The magnetic isotherms were recorded with the external field applied either parallel or perpendicular to the alignment direction of the cylinder samples, which were prepared by aligning powder particles at room temperature in a magnetic field strength of 1 T applied parallel and perpendicular to the cylinder axis and by fixing their direction with epoxy resin. The saturation magnetizations were derived from M–$1/B$ plots based on the high-field data of the magnetization curves. The anisotropy fields were determined from the intersection point of two magnetization curves measured in the magnetic field applied parallel and perpendicular, respectively, to the alignment direction of the cylinder samples.

3. Results and discussion

3.1. Synthesis and structure

From x-ray diffraction analysis it was found that the $Sm_{10}Fe_{85}Ti_x$ compounds annealed at 1473 K for 24 h followed by air quenching exhibit different phases for different Ti contents. The main phase obtained is 1:12 phase for $x \leqslant 4.4$, the 1:7 phase for $4.4 < x \leqslant 4.6$ and the 2:17 phase for $4.6 < x \leqslant 6.5$. In each compound there are some second phases including α–Fe. When the Ti content x is 4.4, the different annealing temperatures and quenching processes led to the appearance of different phases as shown in figure 1. Annealing at 1373 K for 24 h followed by air quenching led to a 2:17 phase (figure 1, curve (a)), whereas annealing at 1473 K followed by air quenching led to a 1:12 phase (figure 2, curve (c)). However, annealing at 1373 K followed by water quenching led to a new 3:29 phase as shown in figure 1, curve (b), just like $Nd_3(Fe,Ti)_{29}$ [13].

X-ray diffraction patterns and the thermomagnetic analysis confirmed that a single-phase $Sm_3(Fe,Ti)_{29}$ compound had been obtained. Therefore it can be concluded that the compound with a single phase of $Sm_3(Fe,Ti)_{29}$ can be obtained by annealing at 1373 K for 24 h, followed by water quenching. The Ti content x which is needed to stabilize the 3:29 phase may vary from 5.0 to 6.5 in the $Sm_{10}Fe_{100-x}Ti_x$ compounds.

Indexation of the powder x-ray diffraction patterns of the $Sm_{10}Fe_{84}Ti_6$ compound was performed on the basis of the $Nd_3(Fe,Ti)_{29}$-type structure with a monoclinic symmetry (space group, $P2_1/c$). The lattice parameters were derived to be $a = 1.065$ nm, $b = 0.858$ nm, $c = 0.972$ nm and $\beta = 96.98°$.

The $Nd_3(Fe,Ti)_{29}$-type structure (3:29), just like the Th_2Zn_{17}-type (2:17) and the $ThMn_{12}$-type (1:12) structures, can be derived by replacement of a fraction of the Ca sites in the $CaCu_5$ structure by a pair of transition-metal atoms (dumbbell) along the hexagonal axis of the $CaCu_5$ structure. The substitution fractions of dumbbell sites in the $CaCu_5$-type structure are $\frac{1}{3}$, $\frac{2}{5}$ and $\frac{1}{2}$ for Th_2Zn_{17}-type, $Nd_2(Fe,Ti)_{29}$-type and $ThMn_{12}$-type structures, respectively.

Figures 2(a), 2(b) and 2(c) are schematic representations of the geometric relationship and the dumbbell substitution sequence projected onto the (110) plane of the $CaCu_5$ structure with a size of $3a_{1:5} \times 3c_{1:5}$ and a thickness of $\sqrt{3}a_{1:5}$ for Th_2Zn_{17}, $Nd_3(Fe,Ti)_{29}$ and $ThMn_{12}$-type structures, respectively. The unit cell of the new $Nd_3(Fe,Ti)_{29}$ structure is indicated by the bold solid lines in figure 2(b).

The $Sm_3(Fe,Ti)_{29}$ compound is a metastable phase at high temperatures. Formation of the single-phase $Sm_3(Fe,Ti)_{29}$ compound requires high-temperature vacuum annealing and rapid quenching in water. The role of the Ti element is to stabilize the structure, as has been found in the $RFe_{11}Ti$ compounds. Because the binary RFe_{12} phase does not exist, a small amount of the third element, such as Ti, V, Cr, Mo, Si or W, is needed to stabilize the 1:12 structure [17, 18].

Figure 3, curves (a) and (b), show x-ray diffraction patterns for the $Sm_3(Fe_{0.933}Ti_{0.067})_{29}$ compound and the nitride. The nitrogen content y was determined to be 5.0. The interstitial phase $R_3(Fe,Ti)_{29}N_{4-\delta}$ was determined on the basis of the structure relationship [19]: $R_3(Fe,Ti)_{29} = R_2Fe_{17}+R(Fe,Ti)_{12}$. The interstitial nitrogen atoms are distributed over two crystallographic sites, namely $4e_1(\frac{1}{3}, \frac{1}{2}, \frac{2}{3})$ and $4e_2(\frac{1}{2}, \frac{1}{4}, \frac{1}{4})$. In the present work the nitrogen amount in the molecular formula is larger than 4; this suggests that the excess amount of the nitrogen may form rare-earth nitride during the nitrogenation, as has been observed in the nitrides of 1:12 structure [17]. By comparison of curves (a) and (b) in figure 3 it can be seen that the $Sm_3(Fe,Ti)_{29}N_y$ compound preserved the same structure as the parent compound, but the diffraction peaks are shifted towards smaller angles, compared with those of the
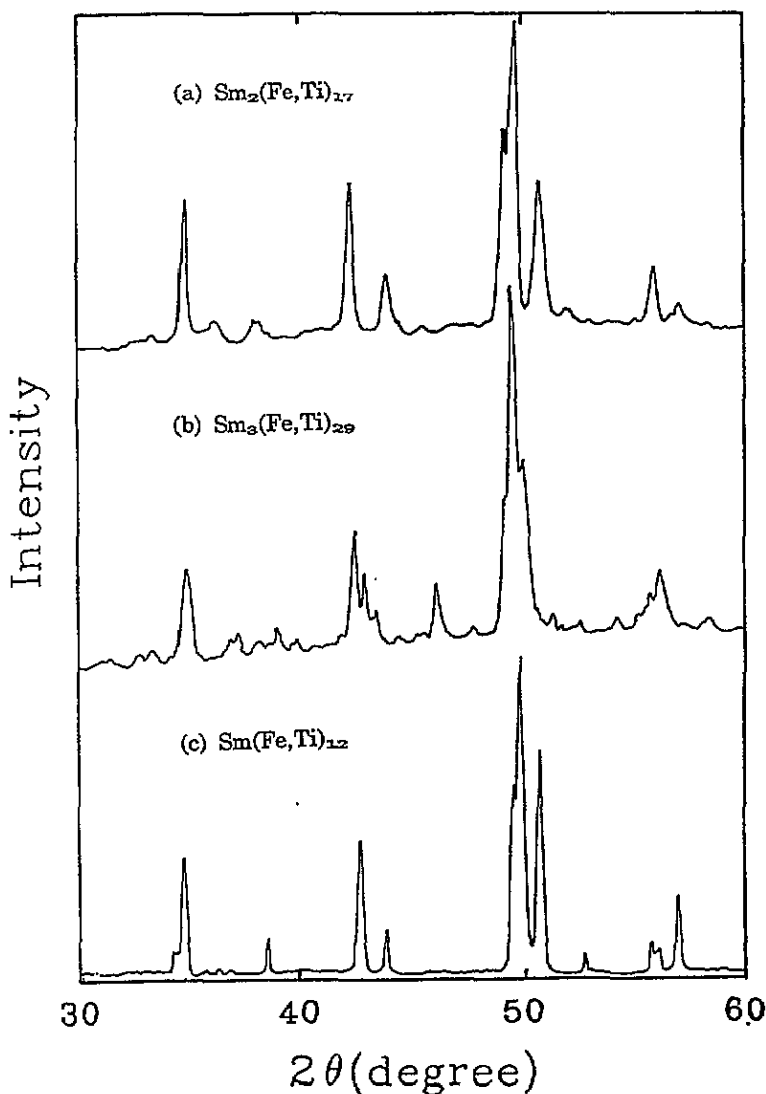
Figure 1. X-ray diffraction patterns (Co Kα) for a $Sm_{10}Fe_{85}Ti_5$ alloy: curve (a), 2:17 phase; curve (b), 3:29 phase; curve (c), 1:12 phase.

parent compound. This suggests that introduction of nitrogen led to an increase in lattice parameters and an expansion in the unit-cell volume. The values of the lattice parameters and the unit-cell volume of the nitride were derived to be $a = 1.098$ nm, $b = 0.882$ nm, $c = 0.985$ nm and $\beta = 97.50°$. The expansion of the unit-cell volume upon nitrogenation is about 7%.

3.2. Magnetic properties

Figure 4 shows the thermomagnetic curves of the $Sm_3(Fe,Ti)_{29}N_y$ and the parent compounds, compared with the Sm_2Fe_{17} compound. The Curie temperature was derived to be 486 K for the parent, which is about 100 K higher than that of the Sm_2Fe_{17} compound [4], and 750 K
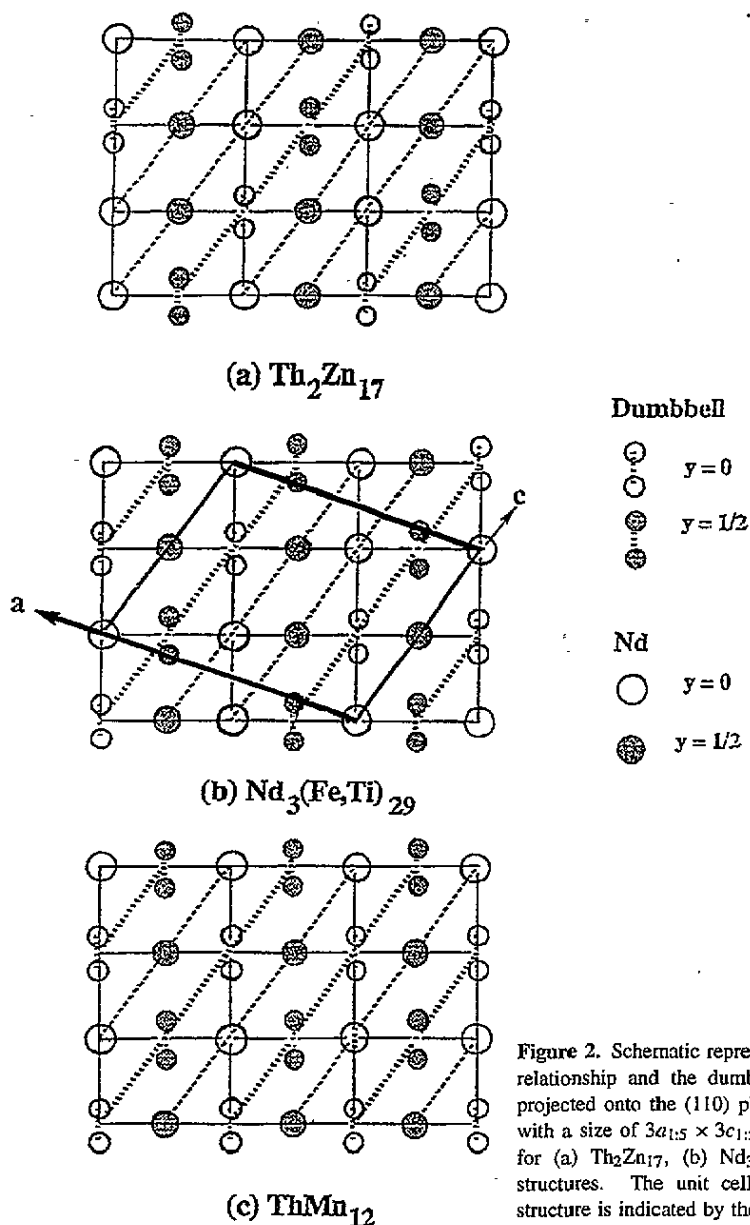
Figure 2. Schematic representation of the geometrical relationship and the dumbbell substitution sequence, projected onto the (110) plane of the $CaCu_5$ structure with a size of $3a_{1:5} \times 3c_{1:5}$ and a thickness of $\sqrt{3}a_{1:5}$ for (a) Th_2Zn_{17}, (b) $Nd_3(Fe,Ti)_{29}$ and (c) $ThMn_{12}$ structures. The unit cell of the new $Nd_3(Fe,Ti)_{29}$ structure is indicated by the bold solid lines in (b).

for the nitride. Introduction of nitrogen led to a distinct enhancement in Curie temperature. In the rare-earth–iron intermetallic compounds, the Curie temperature is dominated by the strength of the exchange coupling between Fe–Fe moments which sensitively depends on the distance between Fe–Fe atoms. A strong increase in Curie temperature upon nitrogenation may partly be explained in terms of the lattice expansion of the nitrides which leads to an increase in the average nearest-neighbour Fe–Fe distance and therefore an increase in the positive Fe–Fe exchange interaction. A theoretical analysis shows that the increase in T_C may also be ascribed to the increase in magnetization upon nitrogenation and the decrease in the spin-up density of states at the Fermi level E_F associated with narrowing of the 3d
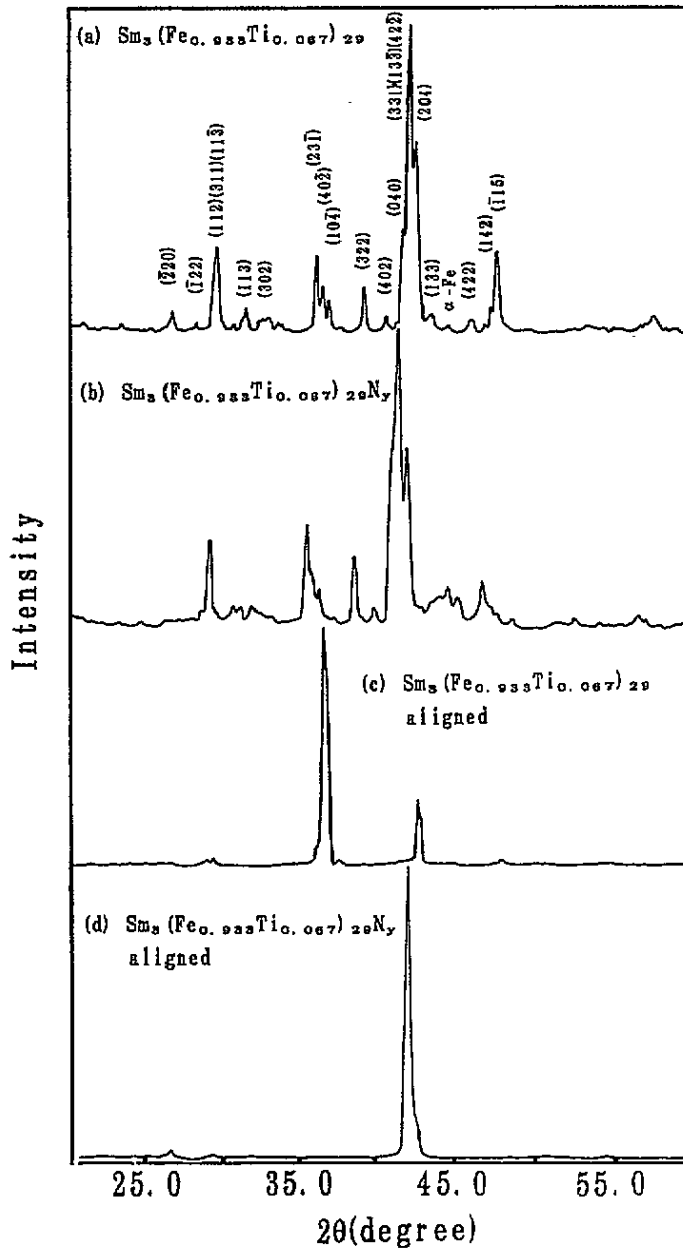
Figure 3. X-ray diffraction patterns (Co Kα) for $Sm_3(Fe,Ti)_{29}$ (curve (a)), $Sm_3(Fe,Ti)_{29}N_y$ (curve (b)), a magnetically aligned powder of $Sm_3(Fe,Ti)_{29}$ (curve (c)) and a magnetically aligned powder of $Sm_3(Fe,Ti)_{29}N_y$ (curve (d)).

band [20].

The high-field magnetization curves of $Sm_3(Fe_{0.933}Ti_{0.067})_{29}N_y$ and the parent compounds are shown in figures 5(a) and 5(b), respectively, which were measured at 4.2 K with external magnetic field strengths of up to 35 T applied either parallel or perpendicular
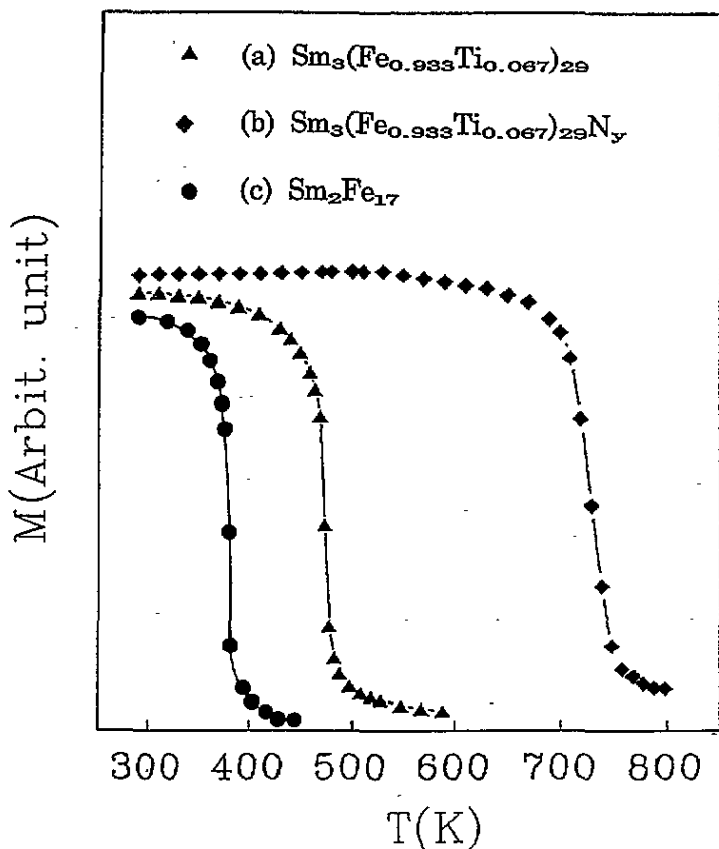
Figure 4. Thermomagnetic curves for $Sm_3(Fe,Ti)_{29}$ ($\blacktriangle$), $Sm_3(Fe,Ti)_{29}N_y$ ($\blacklozenge$) and Sm_2Fe_{17} ($\bullet$) compounds.

to the alignment direction of the samples. The values of the saturation magnetization σ_s were derived by means of σ versus $1/B$ plots to be 160 A m^2 kg^{-1} for the nitride and 140 A m^2 kg^{-1} for the parent compound. Introduction of nitrogen led to an obvious increase in the saturation magnetization. The increase in the saturation magnetization may be associated with the electronic charge transition between Fe and nitrogen atoms [21].

The temperature dependence of the saturation magnetization of $Sm_3(Fe_{0.933}Ti_{0.067})_{29}N_y$ is shown in figure 6. The value of the saturation magnetization either for nitride or for the parent compound decreases monotonically with increasing temperature. At room temperature, $\sigma_s = 140$ A m^2 kg^{-1} for the nitride and 119 A m^2 kg^{-1} for the parent compound.

X-ray diffraction patterns of the magnetically aligned powder samples are shown in figure 3, curves (c) and (d), for the $Sm_3(Fe_{0.933}Ti_{0.067})_{29}$ compound and the nitride, respectively. It can be seen that the (204) line for $Sm_3(Fe_{0.933}Ti_{0.067})_{29}N_y$ is dominant, which is different from the diffraction pattern for its parent compound $Sm_3(Fe_{0.933}Ti_{0.067})_{29}$, where the (402) line is dominant. The small peaks at small angles come from the epoxy resin which was employed to fix the aligned particles in the sample. So the easy magnetization direction is along [102] for the 3:29 nitride and along [201] for the 3:29 parent compound [18] which correspond to the [001] and the [100] directions, respectively, in the superstructure of CaCu$_5$ type as discussed by Shcherbakova *et al* [12]. Introduction of nitrogen led to the occurrence of uniaxial anisotropy in the nitride. From the magnetization curves shown in figure 5(a) it can be seen that the magnetization measured in the field perpendicular to the alignment
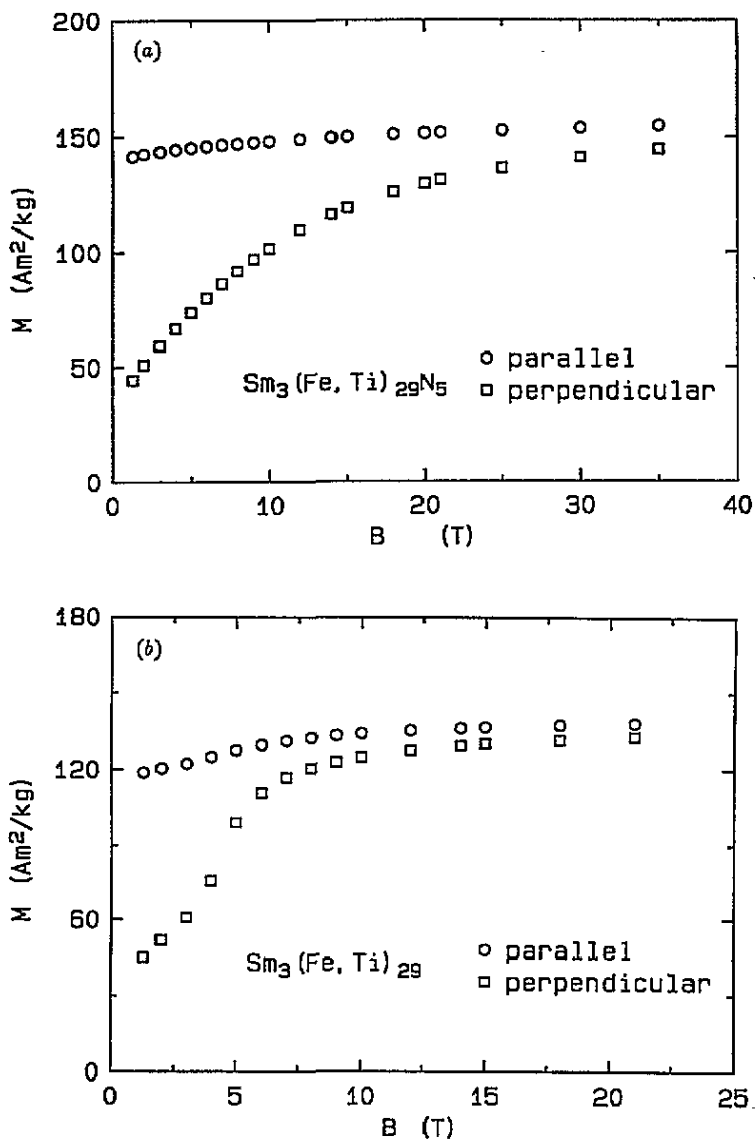
Figure 5. High-field m: · tization curves at 4.2 K for magnetically aligned powder samples for (a) $Sm_3(Fe,Ti)_{29}N_y$ and (b) $Sm_3(Fe,Ti)_{29}$ compounds, with the external magnetic field parallel and perpendicular to the alignment direction.

direction still does not achieve its saturation value even in field strengths up to 35 T. The intersection point of the two magnetization curves by extrapolation gives a B_a-value of 25 T. The temperature dependence of the anisotropy field of the nitride is also shown in figure 6. The anisotropy field B_a decreases monotonically with increasing temperature. At room temperature, $B_a = 12.8$ T. The intrinsic magnetic properties of the $Sm_3(Fe_{0.933}Ti_{0.067})_{29}N_5$ and the parent compound are summarized in table 1.

An interesting feature is encountered in the high-field magnetization curve for the parent compound as shown in figure 5(b). In the magnetization curve measured in a field applied perpendicular to the alignment direction of the sample, a jump-like increase
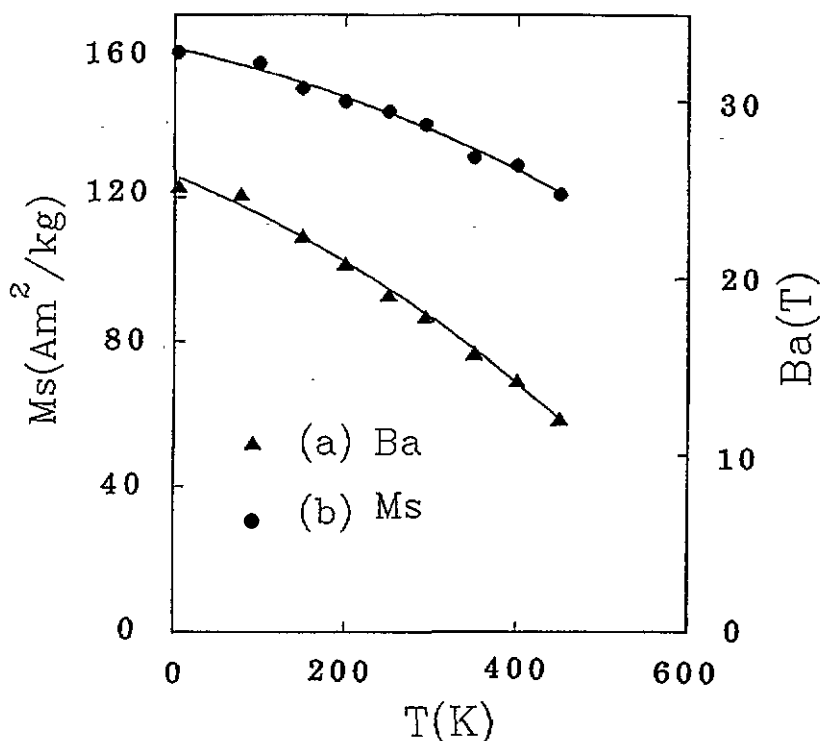
Figure 6. Temperature dependence of the saturation magnetization M_s and the anisotropy field B_a for the $Sm_3(Fe,Ti)_{29}N_y$ compound.

Table 1. Intrinsic magnetic properties of $Sm_3(Fe_{0.933}Ti_{0.067})_{29}$ and $Sm_3(Fe_{0.933}Ti_{0.067})_{29}N_y$.

	T_c (K)	M_s (A m^2 kg^{-1})		B_a (T)	
		4.2 K	293 K	4.2 K	293 K
$Sm_3(Fe_{0.933}Ti_{0.067})_{29}$	486	—	119	—	3.4
$Sm_3(Fe_{0.933}Ti_{0.067})_{29}N_y$	750	160	140	18.1	12.8

in the magnetization can be observed. This phenomenon was also observed in some 1:12-type compounds [17]. These jumps in the isotherms are interpreted as a first-order magnetization process, providing evidence of a field-dependent transition from one spin structure to another.

The hard magnetic properties of the new interstitial nitrides $Sm_3(Fe,Ti)_{29}N_y$ have been investigated by ball milling. Values of the coercivity $\mu_{0i}H_c = 0.83$ T and the energy product $(BH)_{max} = 105$ kJ m^{-3} at 293 K are obtained. These data as the first results of the hard magnetic properties study show that the $Sm_3(Fe,Ti)_{29}N_y$ compound can be developed for permanent magnet application.

4. Conclusions

In conclusion a new interstitial $Sm_3(Fe_{0.933}Ti_{0.067})_{29}$ compound with a monoclinic $Nd_3(Fe,Ti)_{29}$-type structure was obtained by arc melting, followed by annealing at 1373 K

for 24 h and then quenching in water. The interstitial $Sm_3(Fe_{0.933}Ti_{0.067})_{29}N_y$ has the same crystalline structure as the parent compounds. For the nitride, the Curie temperature T_C is 750 K, and the saturation magnetization M_s is 160 A m^2 kg^{-1} at 4.2 K and 140 A m^2 kg^{-1} at room temperature. The nitride exhibits uniaxial anisotropy and the anisotropy field strength is 25 T at 4.2 K and 12.8 T at room temperature. On the basis of the first study on the hard magnetic properties of this new nitride, the magnetic powders with coercivity $\mu_{0i}H_c = 0.83$ T and $(BH)_{max} = 105$ kJ m^{-3} were obtained. The high Curie temperature, large saturation magnetization and strong uniaxial anisotropy make the new interstitial $Sm_3(Fe,Ti)_{29}N_y$ compound a new candidate for permanent magnet application.

Acknowledgments

References

[1]   Sagawa M, Fujimura S, Togawa M and Matuura Y 1984 *J. Appl. Phys.* **55** 2083
[2]   Buschow K H J 1988 *J. Appl. Phys.* **63** 3130
[3]   Zhong X P, Radwanski R J, de Boer F R, Jacobs T H and Buschow K H J 1990 *J. Magn. Magn. Mater.* **86** 333
[4]   Coey J M D and Sun H 1990 *J. Magn. Magn. Mater.* **87** L251
[5]   Yang Y C, Zhang X D, Kong L S, Pan Q and Ge S L 1990 *Proc. 11th Int. Workshop on Rare Earth Magnets and Their Application* vol 2, p 190
[6]   Yang F M, Li Q A, Lu Y, Tang N, Tegus O, Shen B G and Yang L Y 1992 *J. Magn. Magn. Mater.* **114** 255
[7]   Neiva A C, Missel F P, Grich B, Henig E Th and Petzow G 1991 *J. Less-Common Met.* **170** 293
[8]   Hirosawa S, Makida K, Ikegami T and Umemoto M 1992 *Proc. 7th Int. Symp. on Magnetic Anisotropy and Coercivity in Rare Earth–Transition Metal Alloys (Canberra, 1992)* pp 3890–403
[9]   Ohashi K, Osugi R and Tawara Y 1989 *Proc. 10th Int. Workshop on Rare Earth Magnets and Their Applications (Kyoto, 1989)* pp 13–33
[10] Saito H, Takahashi M and Wakiyama T 1988 *J. Appl. Phys.* **64** 5965
[11] Collocott S J, Day R K, Dunlop J B and Davis R C 1992 *Proc. 7th Int. Symp. on Magnetic Anisotropy and Coercivity in Rare Earth Transition Metal Alloys (Canberra, 1992)* pp 437–44
[12] Shcherbakova Ye V, Ivanova G V, Yermolenko A S, Belozerov Ye V and Gaviko V S 1992 *J. Alloys Compounds* **182** 0199
[13] Li H S, Cadogan J M, Davis R L, Margarian A, Dunlop J B and Gwan P B 1994 *Solid State Commun.* **90** 487
[14] Hu Z and Yelon W B 1994 *Solid State Commun.* **91** 223
[15] Rayn D H and Coey J M D 1986 *J. Phys. E: Sci. Instrum.* **19** 693
[16] Gersdorf R, de Boer F R, Wolfrat J C, Muller F A and Roeland L W 1983 *High Field Magnetism* ed M Date (Amsterdam: North-Holland) p 727
[17] Liao L X, Altounian Z and Ryan D H 1991 *J. Appl. Phys.* **70** 6006
[18] Hu J, Wang T, Zhang S, Wang Y and Wang Z 1988 *J. Magn. Magn. Mater.* **70** 22
[19] Cadogan J M, Li H S, Margarian A, Dunlop J B, Ryan D H, Collocott S J and Daris R L 1994 *J. Appl. Phys.* **76** 6138
[20] Jaswal S S, Yelon W B, Hadjipanayis G C, Wang Y Z and Sellmyer D J 1991 *Phys. Rev. Lett.* **67** 644
[21] Zhen Z, Zheng Q, Lei W and Pan C Y 1991 *J. Magn. Magn. Mater.* **104–7** 1157